

A numerical and experimental analysis of the acoustical properties of saxophone mouthpieces using the finite element method and impedance measurements

Maxime Harazi^{a)}

École Normale Supérieure, Paris, France and

Computational Acoustic Modeling Laboratory, McGill University, Montreal, Canada

(Dated: February-July 2012)

The goal of this internship was to analyze and compare the acoustical properties of different saxophone mouthpieces, and provide a method to compute the input impedance of mouthpieces. For this purpose, two different real mouthpieces were modeled and the finite element method (implemented in COMSOL) was used to calculate their acoustical responses. Several methods were investigated to automatically extract accurate mouthpiece geometry data (such as using a coordinate measurement machine) but the data was finally directly measured from molds because of time constraints and because the shapes involved were not too complicated. Then, input impedances of the mouthpieces were measured to validate the simulations. Furthermore, some time was dedicated to configure COMSOL to work on a computer cluster, to perform high performance computing and reduce the simulation times.

Contents	
I Generalities on acoustics and musical acoustics	1
A Classical issues in musical acoustics and goal of this study	1
B The Helmholtz equation	2
C Waves in the mouthpiece	2
D Input impedance	3
E A modelisation of the losses	3
II The Finite Element Method (FEM)	3
A Principles	3
B Cluster computing	5
C A first example : a closed cylinder . . .	5
1 Modeling	5
2 Boundary conditions	6
3 Meshing	6
4 Simulation	6
D A more complex example : a trombone horn	7
III Computing the impedance of saxophone mouthpieces	8
A What is a saxophone mouthpiece ? . .	8
B Getting the geometry of mouthpieces .	9
C On boundary conditions	10
D Results and discussion	11
IV Measuring the impedance of saxophone mouthpieces	11
A The Two Microphone Three Calibration (TMTC) method	11
B Experimental setup	13
C Results and discussion	13

V Conclusions and perspectives	14
Acknowledgments	14

I. GENERALITIES ON ACOUSTICS AND MUSICAL ACOUSTICS

A. Classical issues in musical acoustics and goal of this study

Musical acoustics deals with acoustics of musical instruments and more generally acoustics in a musical context. We can distinguish some different research axes in musical acoustics : some people try to link the subjective perception to the physical properties of instruments and answer questions such as “Are the Stradivarius violins really better than the others ?”¹, others try to synthesize sound using physical modeling or sound processing, some want to optimize existing instruments (to help instrument makers, for example) or create new ones.

In the Computational Acoustic Modeling Laboratory (CAML), McGill University, research is conducted regarding design optimization of wind music instruments (mostly saxophones for now). As better understanding of saxophone acoustics could come from a complete and accurate modelization of the instrument. For the moment, the body of the saxophone is assumed to be a one-dimensional air column with some shape modifications, and the mouthpiece is assumed to be a cylinder of the same volume as a real mouthpiece (this is a low-frequency approximation).

Basically, an auto-oscillating musical instrument can be schematized as in Figure 1 : a source injects energy into a non-linear element, which will then create an oscillation, the latter being amplified thanks to a resonator, which will then interact with the non-linear element. For the saxophone, the source of energy is the musician, who imposes a constant pressure at the entry of the saxophone (the mouthpiece). The non-linear element is a vibrating

^{a)}Electronic address: maxime.harazi@ens.fr

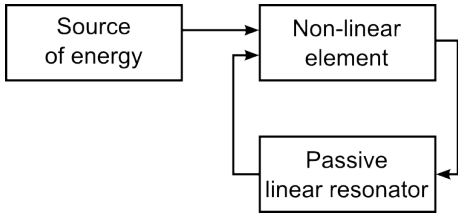


Figure 1. Schematic representation of an auto-oscillating musical instrument

reed attached to the mouthpiece, which transforms the constant pressure from the mouth into an oscillating pressure, thanks to the oscillation of the reed. Finally, the resonator is the body of the saxophone itself.

The goal of this internship was then to develop a method to compute (calculate) the acoustic response of real or imagined saxophone mouthpieces in order to improve the modelization of the complete instrument. For this purpose, two real mouthpieces were modeled in a Finite Element (FE) software, then their responses were calculated. Finally, the responses were measured thanks to a probe, and compared to the computed ones. One can wonder why we want to calculate the acoustic responses, since we can measure them. In fact, it is easy to measure them from the back of the mouthpiece (the side of the neck), but it is very awkward to measure them from the front (the side of the mouth), because of the configuration of the mouthpiece. So the idea is to try to validate the FEM for the calculation of the input impedance seen from the back, since we can make measurements to check the accuracy of the simulations. Once the reliability of FEM to compute the input impedance seen from the back is demonstrated, we assume that it also works fine for the input impedance seen from the front. So at the end, only FEM is used to calculate the input impedance.

B. The Helmholtz equation

To be interested in acoustics means to be interested in the behavior of the pressure field in response to an excitation, and particularly in the behavior of the inducted disturbance, often called the “acoustic” value (acoustic pressure p' , acoustic density ρ' , acoustic temperature T' , ...). Usually, the amplitude of this disturbance is regarded as small compared to the ambient state – without any excitation – which permits us to use a linear approximation in the equations (the “acoustic approximation”). That approximation can be used to derive from the Euler’s equation the well-known “d’Alembert’s equation” – also simply called the “wave equation” – first derived in the one-dimensional version by d’Alembert in 1747 for the case of the vibrating string :

$$\Delta p' = \frac{1}{c^2} \frac{\partial^2 p'}{\partial t^2}. \quad (1)$$

In linear acoustics, that equation is valid for the acoustic pressure p' , but holds for acoustic density ρ' , acoustic

temperature T' and the divergence of velocity $\nabla \cdot \mathbf{v}$.

Since sound is basically just the oscillation of air at a certain frequency, when one studies the acoustical properties of a medium or an object, it is the response to oscillating excitations at different frequencies that is studied. Furthermore, as the wave equation is linear and has time-independent coefficients, the resulting field is expected to be oscillating at the same frequency as the excitation everywhere. Thus, we can assume, using the complex formalism, that p' (simply noted p hereafter) has the form

$$p(\mathbf{r}, t) = \text{Re}(\hat{p}(\mathbf{r})e^{j\omega t}) \quad (2)$$

where ω is the angular frequency of the excitation, and \hat{p} is the complex amplitude of p .

The wave equation (1) is then transformed into the Helmholtz equation

$$\nabla^2 \hat{p} + k^2 \hat{p} = (\nabla^2 + k^2) \hat{p} = 0 \quad (3)$$

with $k = \frac{\omega}{c}$ being the wavenumber and c the speed of sound in air.

That equation governs the spatial dependency of p , which permits us to know p completely, since the temporal part is already known. The goal is then to solve the Helmholtz equation for the frequencies of interest.

C. Waves in the mouthpiece

In saxophones, and in acoustic tubes in general, wave propagation can be described by a set of propagation modes. In the case of a cylindrical duct, all modes except the planar mode are evanescent below a certain frequency (the frequency of the first transverse mode). Considering in a first approximation that mouthpieces have a cylindrical shape, with a radius $r = 1$ cm, it can be shown² that this frequency is approximately given by :

$$f_t = \frac{1.84c}{2\pi r} \sim 10 \text{ kHz} \quad (4)$$

where $c = 340 \text{ m} \cdot \text{s}^{-1}$ is taken.

For frequencies lesser than f_t , the mode is evanescent and then only the plane-wave mode can propagate. Of course, the first propagating transverse mode is well within the range of human hearing (20 Hz – 20 kHz) but excitation of this mode requires transverse circular motion, which will not occur with any significance in musical instruments. Then we now assume that there are only planar waves in the mouthpiece (and in fact we can even assume that this is also true in the whole instrument, since these modes are not well excited and appear at high frequencies). That is, \hat{p} has the form

$$\hat{p} = \underbrace{C_- e^{jkx}}_{\hat{p}_-} + \underbrace{C_+ e^{-jkx}}_{\hat{p}_+} \quad (5)$$

where \hat{p}_- and \hat{p}_+ are the two components of the travelling wave, respectively travelling in the $-x$ and $+x$ direction,

and C_- and C_+ are two complex constants depending on the boundary conditions.

The linearized Euler equation, in the one-dimensional case

$$\frac{\partial u}{\partial t} = -\frac{1}{\rho_0} \frac{\partial p}{\partial x} \quad (6)$$

(ρ_0 being the undisturbed air mass density) now gives us

$$\hat{u} = \frac{1}{Z_c} (\hat{p}_+ - \hat{p}_-) \quad (7)$$

(where $Z_c = \rho c$ is called the characteristic impedance of air).

D. Input impedance

A classical way to characterize acoustic components like mouthpieces or musical instruments is to study their “input impedance” $Z_{in}(f) = \hat{p}_{in}(f)/\hat{u}_{in}(f)$, where \hat{p}_{in} and \hat{u}_{in} are the (complex) acoustic pressure and (complex) air particle velocity at the input of the component. Indeed, the input impedance of a component can give us a lot of information³. Basically, its amplitude quantifies the easiness to set in motion the air thanks to a certain applied oscillating pressure (or a certain applied air velocity). Furthermore, as a complex valued function, the phase of the input impedance gives us information about the relative phase of pressure and velocity, and we can extract from it information like the reflection coefficient, resonant frequencies of the component or even reconstruct its bore⁴.

Let us now calculate the input impedance of a cylinder depending of his load impedance Z_L . We have

$$\begin{aligned} Z_{in} &= \frac{p(0)}{u(0)} \\ &= Z_c \frac{1 + C_-/C_+}{1 - C_-/C_+} \end{aligned} \quad (8)$$

and

$$\begin{aligned} Z_L &= \frac{p(L)}{u(L)} \\ &= Z_c \frac{C_-/C_+ e^{jkL} + e^{-jkL}}{C_-/C_+ e^{jkL} - e^{-jkL}}. \end{aligned} \quad (9)$$

So

$$C_-/C_+ = \frac{Z_L/Z_c - 1}{Z_L/Z_c + 1} e^{-2jkL}$$

which, injected in equation (8), gives

$$Z_{in} = Z_c \frac{Z_L \cos(kL) + jZ_c \sin(kL)}{Z_c \cos(kL) + jZ_L \sin(kL)}. \quad (10)$$

Later, we will use that formula to take into account the effect of an added cylinder at the input of the mouthpieces during measurements.

E. A modelisation of the losses

We now present a model to take into account the losses occurring with acoustic waves⁵. In practice, viscous drag and thermal conduction occur along the mouthpiece walls and cause deviations from ideal (lossless) behavior. Friction along the walls acts to resist the acceleration of air in the mouthpiece and thus decreases the resonant frequencies of the mouthpiece. These effects take place within a thin boundary layer along the bore walls and are carried by vorticity and entropy modes⁵. The thicknesses of the viscous and thermal layers are dependent on the angular frequency ω and the angle of incidence with the bore θ_i and diverge as the frequency goes to zero. As simulations will show, the effect of losses is to reduce the amplitudes and frequencies of the resonant peaks of the input impedance, but we will see that a lossless model is already a fairly good approximation. The modelisation used consists in adding surface admittance Y_s to the walls, given by :

$$Y_s = \frac{1}{2} (1 - i) \frac{\omega}{\rho c^2} [l_{vor} \sin^2 \theta_i + (\gamma - 1) l_{ent}] \quad (11)$$

where

$$\begin{aligned} l_{vor} &= \frac{1}{|k_{vor}|} = \sqrt{\frac{2\mu}{\omega\rho}}, \\ l_{ent} &= \frac{1}{|k_{ent}|} = \sqrt{\frac{2\kappa}{\omega\rho C_p}} = \frac{l_{vor}}{\sqrt{Pr}}, \\ Pr &= \frac{\mu C_p}{\kappa}, \end{aligned}$$

k_{vor} and k_{ent} are the wave number of the vorticity and entropy modes, μ is the dynamic viscosity, C_p is the specific heat capacity, κ the thermal conductivity, and Pr the Prandtl number.

II. THE FINITE ELEMENT METHOD (FEM)

A. Principles

We used the Finite Element Method (“FEM” hereafter) to compute the input impedances of the saxophone mouthpieces. Since this method could require entire books to be presented, and we did not really need to go into the details of it during this internship, we will just present the main ideas necessary to the understanding of our study.

First of all, it is important to know that the FEM relies on the discretization of the domain of interest. That is, the first step consists in meshing the domain. Most commercial FEM software systems include an automatic

mesh generator (mesher), but it is almost always possible to specify some constraints on some sub-domain (for example, one may want to refine the mesh on some very thin part of the domain).

The problem is then expressed in a matricial formulation. The complex initial problem is thus reduced to solving a very big linear system, for which algorithms are well known and implemented in software. There are many FEM software systems, each one being very efficient in one or several domain of physics, and with or without a model builder and an automatic mesher.

The software used is ‘‘COMSOL Multiphysics’’ (formerly called ‘‘FEMLAB’’). It is a commercial software which has the advantage of permitting cluster computing. Models from CAD softwares like SolidWorks and CATIA can be imported into COMSOL but it requires an additional (paying) module. One of the most interesting features in COMSOL is that different fields of physics can be coupled. For example one can be interested in the stresses in the reed in addition to the acoustics of the saxophone mouthpiece. We would then use the ‘‘Acoustics’’ and ‘‘Structural Mechanics’’ modules and couple them. In this study, we only used the ‘‘Acoustics’’ module, because we considered the reed as non-vibrating.

We have

$$\nabla^2 \hat{p} + k^2 \hat{p} = 0. \quad (12)$$

We multiply it by a scalar function ϕ and integrate it over the domain Ω :

$$\int_{\Omega} \phi [\nabla^2 \hat{p} + k^2 \hat{p}] d\Omega = 0. \quad (13)$$

We now use the chain rule $u \nabla \cdot \mathbf{A} = \nabla \cdot (u \mathbf{A}) - \nabla u \cdot \mathbf{A}$ with $\mathbf{A} = \nabla \hat{p}$ and $u = \phi$ to obtain

$$\int_{\Omega} \nabla \cdot (\phi \nabla \hat{p}) d\Omega - \int_{\Omega} \nabla \phi \cdot \nabla \hat{p} d\Omega + \int_{\Omega} \phi k^2 \hat{p} d\Omega = 0. \quad (14)$$

The use of the divergence theorem gives

$$\int_{\Gamma} \phi \nabla \hat{p} \cdot \mathbf{n} d\Gamma - \int_{\Omega} \nabla \phi \cdot \nabla \hat{p} d\Omega + \int_{\Omega} \phi k^2 \hat{p} d\Omega = 0. \quad (15)$$

But equation (6) gives $j\omega \hat{u} = -\frac{1}{\rho_0} \nabla \hat{p}$, so we have

$$-\int_{\Gamma} \rho_0 j\omega \hat{u}_n \phi d\Gamma - \int_{\Omega} \nabla \phi \cdot \nabla \hat{p} d\Omega + \int_{\Omega} \phi k^2 \hat{p} d\Omega = 0, \quad (16)$$

where \hat{u}_n is the normal velocity on the surface Γ . When computing an input impedance, the normal velocity is zero everywhere on Γ except on the exciting surface, on which it is an arbitrary constant.

The next step in the FEM consists in introducing a ‘‘basis’’ on which we can decompose the functions ϕ and \hat{p} . So, as we are only interested in the values at the nodes of the mesh, we choose a basis function Ψ_i for each node

i . For example, in the one-dimensional case, the simplest choice is to take Ψ_i as a piecewise linear function, with $\Psi_i(i) = 1$, $\Psi_i(i-1) = 0$ and $\Psi_i(i+1) = 0$. Other common used functions are piecewise quadratic or higher orders polynomials.

So we have

$$\begin{cases} \phi \approx \phi_{\text{FEM}} = \sum_i \phi_i \Psi_i(x, y, z) \\ \hat{p} \approx \hat{p}_{\text{FEM}} = \sum_i \hat{p}_i \Psi_i(x, y, z) \end{cases} \quad (17)$$

which injected in the previous equation gives (using the Einstein notation)

$$-\phi_i \rho_0 j\omega \int_{\Gamma} \hat{u}_n \Psi_i d\Gamma - \phi_i \hat{p}_j \int_{\Omega} \nabla \Psi_i \cdot \nabla \Psi_j d\Omega + \phi_i \hat{p}_j k^2 \int_{\Omega} \Psi_i \Psi_j d\Omega = 0. \quad (18)$$

Then, assuming that $\forall i, \phi_i \neq 0$,

$$-\rho_0 j\omega \int_{\Gamma} \hat{u}_n \Psi_i d\Gamma - \hat{p}_j \int_{\Omega} \nabla \Psi_i \cdot \nabla \Psi_j d\Omega + \hat{p}_j k^2 \int_{\Omega} \Psi_i \Psi_j d\Omega = 0. \quad (19)$$

Let us now define the matrices

$$M_{ij} = k^2 \int_{\Omega} \Psi_i \Psi_j d\Omega \quad (20)$$

and

$$K_{ij} = \int_{\Omega} \nabla \Psi_i \cdot \nabla \Psi_j d\Omega \quad (21)$$

and the vector

$$F_i = -\rho_0 j\omega \int_{\Gamma} \hat{u}_n \Psi_i d\Gamma. \quad (22)$$

Doing this, we can now rewrite (19) in a matrix formulation

$$M_{ij} \hat{p}_j - K_{ij} \hat{p}_j = F_i \quad (23)$$

or

$$[M - K] \begin{pmatrix} \vdots \\ \hat{p} \\ \vdots \end{pmatrix} = F. \quad (24)$$

Now, it is important to note that M , K , and F are totally known, and the only unknown is the vector $\begin{pmatrix} \vdots \\ \hat{p} \\ \vdots \end{pmatrix}$.

The goal is then to solve a simple but big linear system, which is possible thanks to computers and algorithms adapted to FE problems.

After having solved the system, we know the pressure field in the domain, but only for the nodes of the mesh. So if one is interested in the pressure at a point which is not a node of the mesh, interpolation between known points is needed. Many interpolating functions can be chosen, but in most cases polynomials are used and give good results. In this study, we always used quadratic interpolating functions.

B. Cluster computing

As we said, COMSOL can be used on a computer cluster to reduce the simulation times. As part of a consortium called CLUMEQ, itself in the “Calcul Quebec/Compute Canada” networks, McGill University has access to several clusters. We used one called “Colosse”, which is located in the city of Quebec, and has 960 nodes, each with 8 processor cores (7680 cores total) and 24 gigabytes of RAM (23 TB total). Basically, a computer cluster is just a super-computer with a lot of processors and RAM. There are several public clusters in most of the countries. In June 2012, in the list of the 500 most powerful computer systems⁶, we can find that Canada has ten computer clusters, France has twenty-two and USA has two hundred fifty two. At this date “Colosse” is ranked 314, with 77.2 TFLOPS \cdot s⁻¹ (77.2 \cdot 10¹² FLoating point Operations Per Second).

The most interesting usage of cluster computing in our case is the possibility to distribute a parameter on several nodes. For example, if we want to run a simulation with an excitation frequency varying between 0 Hz and 10 kHz, we can launch our simulation on ten nodes, each node computing the input impedance on a 1 kHz-range (for example the first node will run the simulation in the range 0 Hz – 1 kHz, the second node in the range 1 Hz – 2 kHz, and so forth). We would then expect a simulation time proportional to (number of nodes)⁻¹. Figure 2 presents the results of a benchmark on a simulation and confirms what we just said. Almost all our simulations were run on eighty cores, reducing the simulation times by a factor ten compared to simulations run in the laboratory.

C. A first example : a closed cylinder

Let us now study a first example to detail the procedure of computing an input impedance thanks to COMSOL. One of the easiest systems to study in acoustics is probably a closed cylinder – here “closed” means one side excites the air inside the cylinder (with an incident pressure field), and the other side is closed by a rigid wall. Furthermore, in our particular case, it is a good choice for two reasons : 1) we can calculate exactly its resonant frequencies, and then estimate the accuracy of the simulations; 2) we can model it in a two-dimensional model, which greatly improve the running time of the simulation.

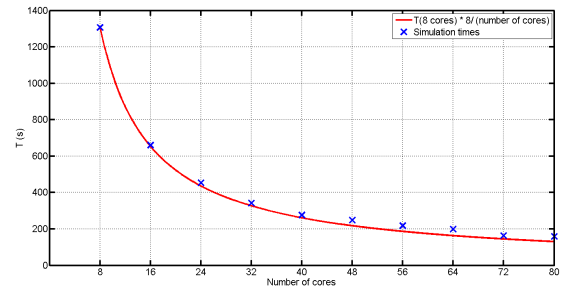


Figure 2. Simulation times depending on the number of cores used and comparison with the expectation that the simulation time should be proportional to (number of cores)⁻¹.

That is why we decided to model a cylinder of length 1 m and radius 10 cm.

1. Modeling

Since there is a revolution symmetry around the axis of the cylinder, which implies that what happens in a section of the cylinder is independent of the section, we can limit our calculations to a two-dimensional model. Of course, this symmetry is true only because we will excite the cylinder with a planar wave. Furthermore, we can also limit our model to a half section, and impose the normal-velocity to be zero on the central axis. Finally, our model just consists in a rectangle whose dimensions are the radius and length of the cylinder.

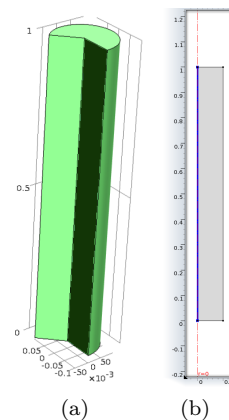


Figure 3. Using the symmetries of the model to reduce the simulation times : (a) Three-dimensional original model (b) Two-dimensional reduced problem which consists of a half section (dark green in the 3D model) of the cylinder.

On one node, the simulation of the two-dimensional case, from 0 Hz to 1 kHz, with a 1 Hz step takes 12 s, whereas it takes 74 s in the three-dimensional case.

2. Boundary conditions

We now have to choose the boundary conditions for each of the four sides of the rectangle. Since we want to calculate the input impedance of the cylinder, we need to choose one of the extremities of the rectangle to inject a planar wave into the cylinder. Notice here that it implies the exciting wall is considered as a closed end, since an opened end would lead to a vanishing pressure. On the three other sides, we impose a ‘‘Hard boundary wall’’ condition, since we want to modelize a closed cylinder. Later, we will want to add some losses so we will need to change these boundary conditions (adding the wall admittance (11)).

3. Meshing

The last step before effectively running the simulation is the meshing of the model. Thankfully, COMSOL comes with an automatic mesh generator, and we do not need to really worry about the mesh. It is possible to select a default mesh quality, or to choose some of its parameters (like the minimal or maximal size of the elements, the maximum growing factor, ...). In two dimensions, the elements consist of triangles, and in three dimensions these are tetrahedra. The mesh used here consists of 2606 elements (triangles).

It is important to fully resolve the waves in space. In practice, it is recommended to use a maximum mesh element size that provides about five 2nd-order elements per wavelength. At the maximum frequency studied here (2500 Hz) the wavelength is 14 cm.

4. Simulation

Now that we have the complete model, we can run the simulation. In fact, since we are looking for the input impedance, which is a frequency-dependent function, we will run one simulation for each frequency we want. That is, if we want $Z(f)$ from 0 Hz to 1 kHz, with a resolution of 1 Hz, we will run 10000 simulations. Of course COMSOL can deal with it and we do not need to launch every simulation manually.

Once the simulation is finished we can ask COMSOL to extract the value \hat{p}/\hat{v} , on the excited side, that is, the input impedance of the cylinder. Figure 4 shows the input impedance with and without losses (two different simulations). As explained before, losses were implemented thanks to the admittance (11).

To check the accuracy of the simulation, we can calculate the resonant frequencies of the cylinder. In fact, whether the non-excited end of the cylinder is opened or closed, a certain part of the input pressure wave will reflect at this end and comes back, then reflects again, and so forth. This gives rise to standing waves. If the returning wave is in phase with the driving wave, it will create a very big pressure at the input, giving birth to a maximum of $|Z_{in}|$ (we call this a resonance). On the contrary, if the returning wave is out of phase with the

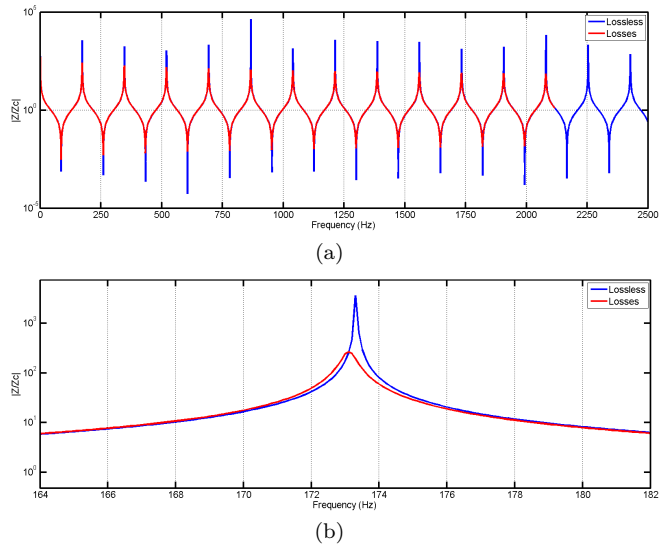


Figure 4. (a) Computed input impedance of a closed cylinder, with and without losses. The length is one meter and radius ten centimeters. (b) Zoom around the first resonance. Notice that losses decrease amplitudes and frequencies of the resonances.

driving wave, the two waves will annihilate at the input, then creating a minimum of $|Z_{in}|$ (we call this an anti-resonance). One important thing to notice is at the corresponding frequencies (resonance or anti-resonance) the imaginary part of the input impedance vanishes, so it is easy to extract them. Indeed, according to equation (5) we have

$$\frac{\hat{p}_-(0)}{\hat{p}_+(0)} = \frac{C_-}{C_+}. \quad (25)$$

For a resonance, this number is real, and for an anti-resonance, it is imaginary. But in both cases, equation (8) leads us then to the fact that Z_{in} is real.

Furthermore, the theoretical resonant frequencies of a closed cylinder are well-known and given by

$$f_n = \frac{c}{2L}n \quad (26)$$

where $n = 1, 2, 3, \dots$

Table I gives the resonant frequencies extracted from the simulations, with and without losses and the theoretical frequencies. We can see that the simulations seem quite accurate, since the maximum relative error is 10^{-3} . When losses are taken into account, COMSOL uses a non-linear solver, which greatly increases the simulation time. Furthermore, for some frequencies, solutions may not be found (for example, 13th and 14th harmonics could not be resolved). Finally, even if it seems that in this case the losses do not change very much the behavior of the waves (at least for the resonant frequencies), we will see that the effect of the losses becomes important as the dimensions of the object studied decrease.

n	COMSOL without losses (Hz)	COMSOL with losses (Hz)	Theoretical frequency (Hz)
1	173.38	173.11	173.32
2	346.67	346.33	346.63
3	519.95	519.58	519.95
4	693.23	692.84	693.26
5	866.50	866.12	866.58
6	1039.96	1039.41	1039.89
7	1213.21	1212.72	1213.21
8	1386.79	1386.05	1386.52
9	1560.17	1559.40	1559.84
10	1733.48	1732.78	1733.15
11	1906.85	1906.18	1906.47
12	2080.34	2079.61	2079.78
13	2253.86	-	2253.10
14	2427.34	-	2426.41

Table I. Comparison between theoretical and simulated (with and without losses) resonant frequencies of a closed cylinder of length $L = 1$ m. The 13th and 14th harmonics could not be resolved in the case with losses, because solutions were not converging.

To conclude this initial analysis of simulations with COMSOL, let us talk about some important technical considerations. One important thing to have in mind is that COMSOL has actually calculated the pressure field in the whole domain (even if we are only interested in the pressure field on a very little sub-domain of the whole model), and for every frequency. One consequence is that the output file of a simulation running from 0 Hz to 5 kHz, with a 0.1 Hz frequency step can be very big : from 10 GB to 60 GB, depending on the size of the model and quality of the mesh (i.e. the number of pressure values stored for each frequency). That is a thing to consider seriously since saving a 60 GB file can take a few hours, and almost the same time for opening it ...

D. A more complex example : a trombone horn

To complete our initiation of the computation of input impedance with COMSOL, we had the opportunity to participate in a PhD thesis conducted at IRCAM (Paris, France) by Pauline Eveno. Her thesis is about the characterization of brass instruments and a part of it is focused on the comparison of different numerical methods to evaluate the input impedance of horns. It is part of a project called PAFI⁷ aimed at helping craftsmen to design and characterize their musical instruments.

Pauline gave us the profile of a trombone horn and asked us to calculate its input impedance using COMSOL. An important difference compared to the previous example of the closed cylinder is that we were asked to calculate the input impedance with an open end condition. That is, the horn is radiating in the ambient air. To modelize such a thing, we had to surround the horn with a big sphere of air and used the “spherical wave radiation” (anechoic) boundary condition, which “allows an outgoing wave to leave the modeling domain with minimal reflections” (COMSOL documentation). Of course,

this implies that the studied domain is greatly larger than in the closed case, but once again, symmetries could be used. Indeed, a trombone horn presents a revolution symmetry, so a two-dimensional model was used. Finally, the model used consists of a half section of the horn, and a hemisphere (see figure 5).

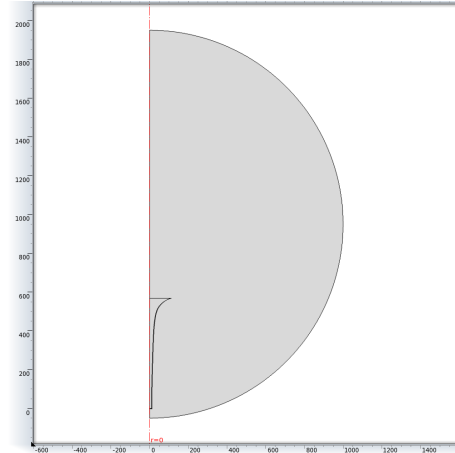


Figure 5. Model used for the trombone horn. Once again, the revolution symmetry permits us to greatly reduce the domain.

Figure 6 shows the mesh used for the simulation. This mesh was automatically generated thanks to the COMSOL’s mesher, and contains 14731 elements.

A 0.1 Hz frequency step was used, and the simulation took approximately four hours in the lossless case (far more in the lossy case), on eight cores (we used the fastest computer in the laboratory, a 12-core Mac Pro with 32 GB of RAM). We could not run the simulation on Colosse, because the output file was too big to handle (60 GB): saving the file on Colosse took approximately three hours, and opening it in the laboratory one hour (plus one hour to download the file from Colosse to the laboratory), so it was faster to run the simulation on a less powerful computer, without saving the output file (just reading it).

Exactly like in the previous case of the cylinder, once the simulation is complete, we can then extract the input impedance. Figure 7 shows the input impedance with and without losses.

One nice thing in the case of the trombone horn is we could compare our method with others. Indeed, Pauline contacted different teams using different methods and asked them to compute the input impedance of the horn^{8,9}. Figure 8 shows the input impedance computed thanks to FEM (our simulation), Transmission Matrix Method with spherical elements (TMM) and the software Sysnoise in two different modes (3D or 2D axisymmetric). The Sysnoise simulations were conducted by Thierry Scotti and Philippe Herzog (Laboratoire de Mécanique et d’Acoustique, Marseille).

We can see that our simulation seems to compare well with the measured data and most of the other methods. The discrepancies can come from some error in the model of the horn, or noise in the measure.

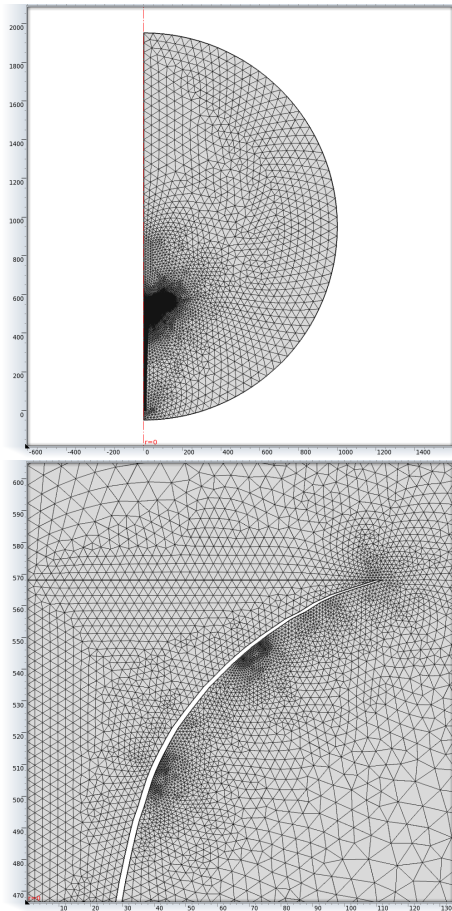


Figure 6. Mesh used for the computation of the input impedance of a trombone horn.

III. COMPUTING THE IMPEDANCE OF SAXOPHONE MOUTHPIECES

Now that we know how to use COMSOL to compute input impedances, let us focus on saxophone mouthpieces. As we said in the introduction, the goal is to compute their input impedances. But we will see that measuring it is a tricky procedure, so we will be – at least to begin with – interested in the impedance seen from the back of the mouthpiece, rather than from the front (see figure 9) – we will call it respectively “input impedance seen from the back” and “input impedance seen from the front”. That will allow us to check our simulations thanks to measurements. In a second stage, after having checked the simulations are coherent with the measurements, the next step is to compute the “real” input impedance – that is seen from the mouth – assuming that if our method is reliable for computing input impedance from the neck side, it is also reliable for computing it from the mouth side.

A. What is a saxophone mouthpiece ?

As we said in the first part, the saxophone mouthpiece is the key element that permits a player to create oscil-

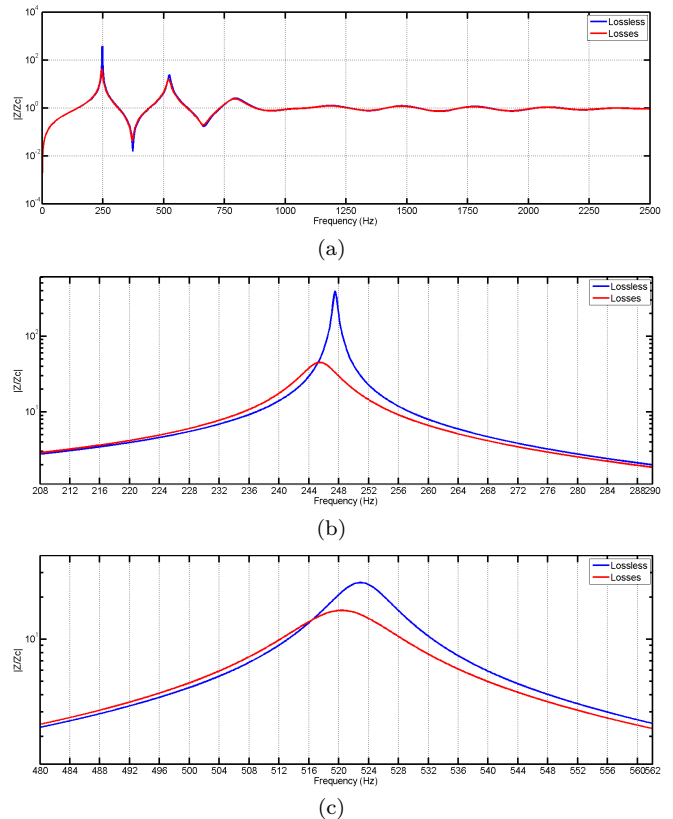


Figure 7. (a) Simulated input impedance of a trombone horn, with and without losses. (b) Zoom around the first resonance. (c) Zoom around the second resonance. Notice that losses decrease amplitudes and frequencies of the resonances. In both cases a 0.1 Hz frequency step was used.

lations from the constant pressure in his mouth. These oscillations, generated by the non-linear behavior of the reed, will then be injected into the body of the saxophone and resonate to radiate and finally create sound.

There are a lot of different saxophone mouthpieces on the market. Each mouthpiece can differ from others mostly by the material it is made of (ebonite, metal, plastic, ...), its length, or internal geometry (see figure 9). We measured the input impedances seen from the back for five different mouthpieces : Lebayle Jazz Chamber MMA 7*, Selmer C*, Caravan, Meyer 5M, and Meyer 6M. But since it required a lot of time to model a single mouthpiece, only the first two ones were modeled. The Lebayle mouthpiece is shown on Figure 10.

The internal structure of a saxophone mouthpiece is mainly made of three parts : 1) from the neck, it begins with a cylindrical section, the radius being almost always of 8 mm, since a certain standard is needed to adapt them on every saxophone 2) then there is an intermediate section of various shape (semi-hemispherical for the Selmer C*, for example; cylindrical for the Lebayle mouthpiece) 3) and finally, a more rectangular section ends the mouthpiece.

Figure 11 shows how the mouthpiece is inserted in the mouth. The lower lip is pressing the reed, introducing

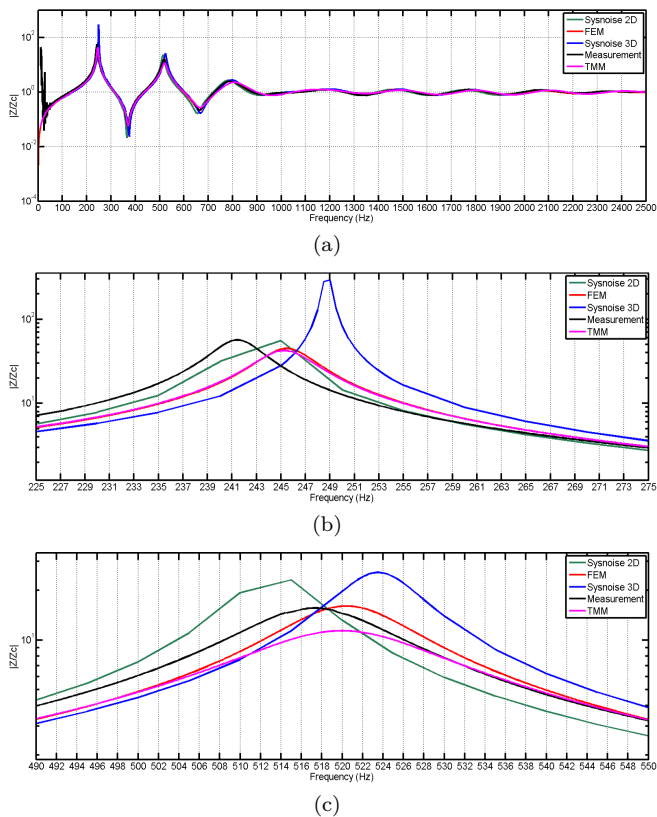


Figure 8. (a) Simulated input impedance of a trombone horn, thanks to different methods, and comparison with measurement. (b) Zoom around the first resonance. (c) Zoom around the second resonance.

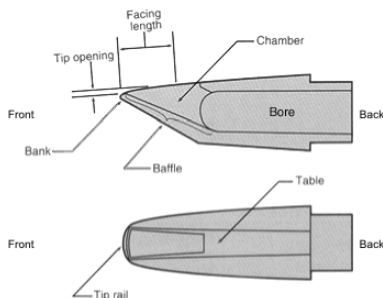


Figure 9. Structure of a saxophone mouthpiece

some damping in the vibration of the latter.

B. Getting the geometry of mouthpieces

One critical step in our study is the modeling of the mouthpieces. Indeed, this is almost the only input data we have to provide to COMSOL, and since we want to study the effects of differences in internal geometry of mouthpieces on their input impedances, we had to create fine models of their interiors.

The first step was then to create molds of the interiors of the mouthpieces. We made two molds of two different



Figure 10. One of the mouthpieces modeled : the Lebayle Jazz Chamber MMA 7*

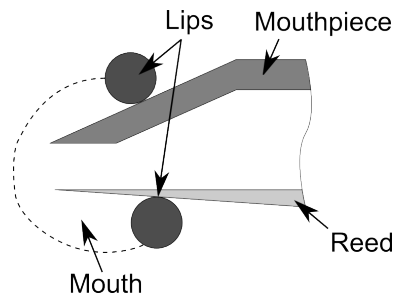


Figure 11. Mouthpiece in the mouth

mouthpieces : the famous Selmer C*, and the Lebayle Jazz Chamber MMA 7*. The molds were made in silicone.

Then, we had to model the molds in COMSOL. For doing this, one first approach was to try to use a machine of the mechanical engineering department. This machine takes pictures of the object and then creates a three-dimensional model of its exterior. Even if it works fine, we were unable to export the model in a format supported by COMSOL.

We also tried to contact the manufacturers, Selmer and Lebayle (French companies). Jérôme Selmer was very interested in our study but did not want to share his data with us, because of the short duration of the internship. We hope a collaboration will be possible in a near future between CAML and Selmer. Unfortunately, Lebayle did not answer us.

Finally, we resigned to use the COMSOL model builder



Figure 12. Silicone molds were used to get the internal geometry of the mouthpieces. From top to bottom : the mold corresponding to the Selmer mouthpiece, and that corresponding to the Lebayle mouthpiece.

and manual measurements. Even if there are fewer possibilities than in a dedicated design software like Solidworks or CATIA, we succeeded – thanks to the help of mechanical engineering students – in making respectable models. Let us note here that silicone is not the best choice for manual measurements, because of its softness.

Figures 13 and 14 show the models made for the two mouthpieces.

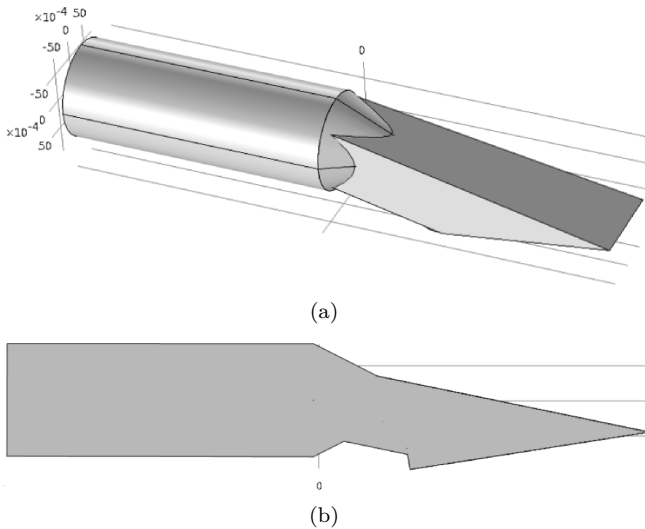


Figure 13. Model of the interior of the Selmer C* mouthpiece : (a) Three-dimensional view (b) Sectional view

Figure 15 shows the automatic mesh generated by COMSOL (finest automatic resolution was chosen) and table II gives some characteristics of the two models.

C. On boundary conditions

Once the model is ready, we need to set up the boundary conditions. As we said, since we only know how to measure impedance from the back of the mouthpiece, we choose the end of the mouthpiece (a disk, in fact) as the

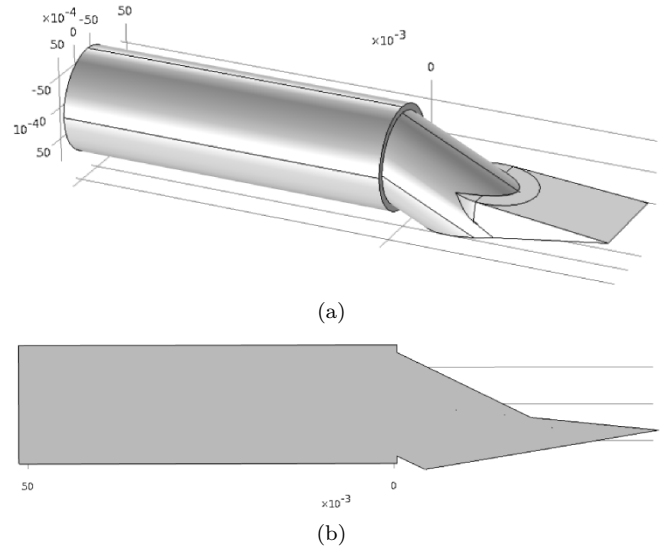


Figure 14. Model of the interior of the Lebayle Jazz Chamber MMA 7* mouthpiece : (a) Three-dimensional view (b) Sectional view

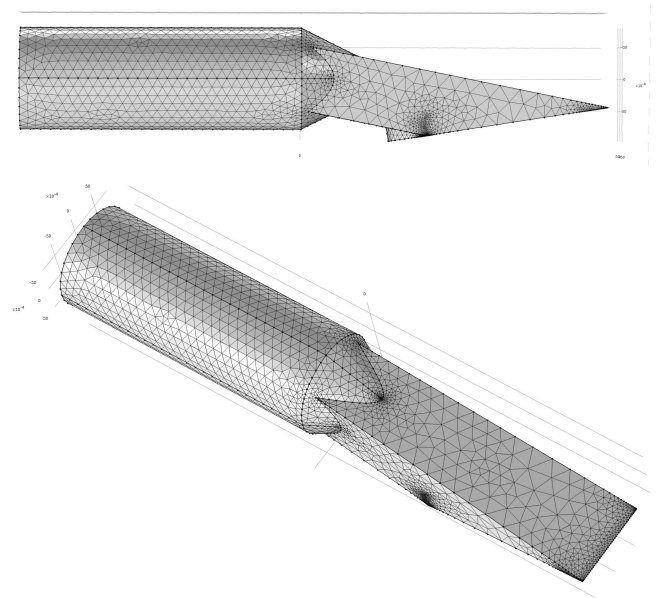


Figure 15. Meshing of the Selmer C*

exciting side. Then, since it is easier to model a closed mouthpiece (that is, the reed is pushed against the table), we decided to model that configuration. It should be emphasized here that this study concerned the static acoustic response of the mouthpiece and not the complex aeroacoustic behavior of the mouthpiece under normal dynamic playing conditions, when the reed is moving back and forth. Thus, this is not a normal playing configuration (there is a little space between the reed and the table when the musician is not playing), but since we wanted to validate our method in a first stage, we decided to choose the easiest configuration. Finally, apart from the exciting side, on which the “Incident pressure

	Selmer	Lebayle
Volume	$1.32 \cdot 10^{-5} \text{ m}^3$	$1.30 \cdot 10^{-5} \text{ m}^3$
Number of elements	54154	36392
Number of degrees of freedom solved for	77797	53813
Meshing time	7.15 s	5.42 s

Table II. Some characteristics of the two models we made.

field” condition is applied, all of the boundaries of the mold are considered as “Hard boundary walls”.

D. Results and discussion

For each mouthpiece, one first simulation was run, with a 10 Hz frequency step, to locate the resonances. Then a second simulation was run with a 0.1 Hz frequency step, but only around the resonances. The final input impedance is then extracted doing the “union” of the two simulations. The total simulation times are 2300 s and 4500 s for the Lebayle and Selmer mouthpieces respectively. The saving times are 1500 s and 2500 s. Finally, computing the input impedances took respectively something like 1 h and 2 h.

Figure 16 shows the input impedance of the Lebayle mouthpiece, with and without losses, and a zoom around the first resonance (found to be at 2556 Hz in the lossless case and 2539 Hz in the lossy case).

Figure 17 shows the same graph for the Selmer mouthpiece. The first resonance was found to be at 2227 Hz in the lossless case and 2210 Hz with losses considered.

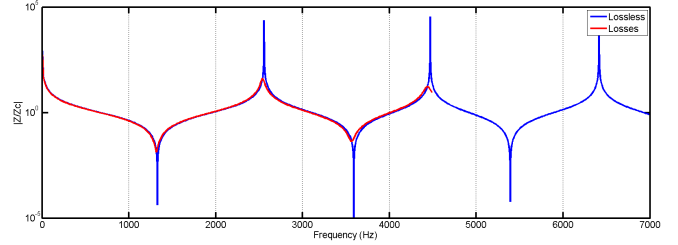
We can show that these values are reasonable. Indeed, since the volumes of the mouthpieces are known, we can calculate the first resonant frequencies for cylinders of equivalent volumes, and same radius. This leads approximately to 2600 Hz, so we can say that our simulation results are in the right ballpark.

Finally, in cases with losses, a 0.1 Hz frequency step is not really necessary, since in this case the resonant peaks are not very sharp. However, such a resolution is required in the lossless case, in order to get a reliable estimation of the resonant frequencies and amplitudes.

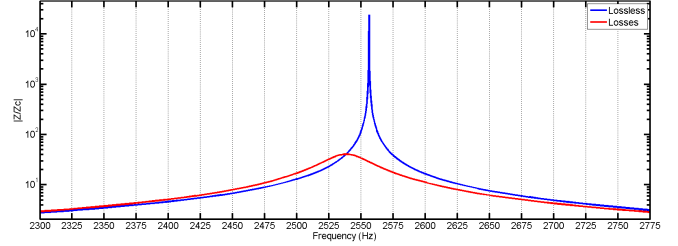
IV. MEASURING THE IMPEDANCE OF SAXOPHONE MOUTHPIECES

Now that we have computed the input impedances of the two mouthpieces, we want to see if our simulations are coherent with measurements, in order to validate the method.

There are many different methods to measure input impedances^{10–12}. We used a viariant of the Two Microphone Three Calibration (TMTC) method.

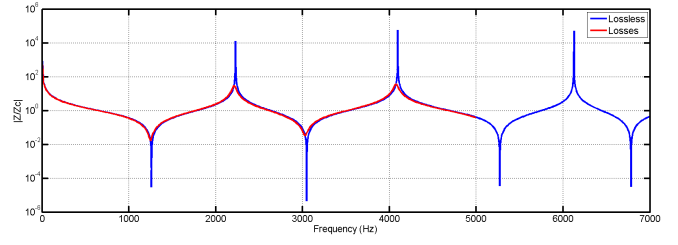


(a)

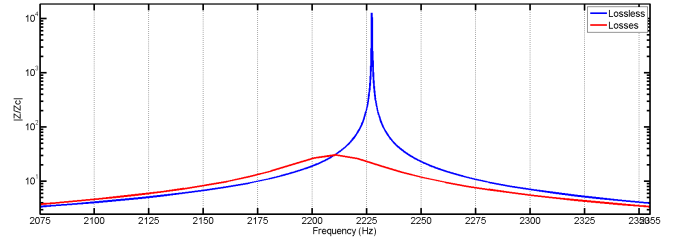


(b)

Figure 16. (a) Simulated input impedance of the Lebayle mouthpiece, with and without losses. (b) Zoom around the first resonance (2556 Hz in the lossless case and 2539 Hz with losses). A resolution of 0.1 Hz was used around the resonances, and 10 Hz otherwise.



(a)



(b)

Figure 17. (a) Simulated input impedance of the Selmer mouthpiece, with and without losses. (b) Zoom around the first resonance (2227 Hz in the lossless case and 2210 Hz with losses). A resolution of 0.1 Hz was used around the resonances, and 10 Hz otherwise.

A. The Two Microphone Three Calibration (TMTC) method

To get the input impedance of an acoustical component, the basic idea is to measure pressure and particle velocity at the input, while the component is excited at a certain frequency. But measuring the particle velocity is in fact quite tricky and while pressure sensor

measurements are robust and well developed because of the broad utility of microphones, there are few equivalent probes to directly measure particle and volume velocity. Flow can be measured directly using something like a hot-wire anemometer, but for small geometries the probe usually disturbs the flow, thus rendering the measurement inaccurate. One method which requires only microphones is the Two Microphone Three Calibration (TMTC) method¹³. That method assumes the waves involved are planar (no transverse mode), which is a good approximation in our situation (see I.C). We will now present the main aspects of the method.

Let us consider the experimental setup presented in Figure 18 : a “measurement head” made of brass is attached to the acoustic component under study (a mouthpiece, in our case). Two microphones are connected to the measurement head, in order to measure the pressure in two specific places. Let us call the plane between the measurement head and the acoustic component the “reference plane”. A loudspeaker can send an acoustic signal into the measurement head.

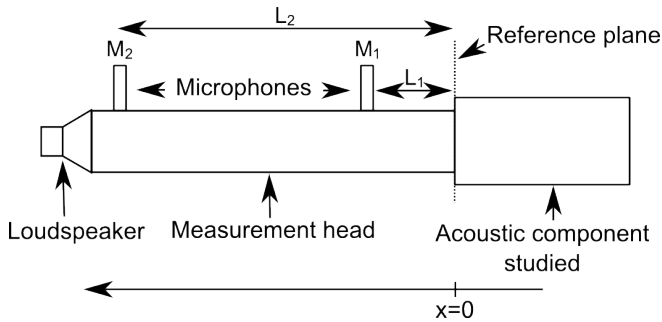


Figure 18. Principle of the Two Microphone Three Calibration (TMTC) method : two microphones measure pressure in a measurement head, at the end of which the component to be studied is attached. At the other end a loudspeaker is sending a signal.

Let us now just cite the authors, because their explanation is quite clear and does not need reformulation :

We first assume that the excitation is monochromatic and study the response of the system at a single frequency. We also assume that the neck of the acoustical cavity to be studied is almost cylindrical and that, inside this neck, the acoustical wave contains only one single transverse mode; in other words, in this region, the propagation of the acoustical wave is equivalent to a one dimensional problem, so that the solution of the wave equation can be obtained (in theory) from the value of the acoustical field and its space derivative at one point (as in quantum mechanics, for example, where the solution of the Schrödinger equation in a one-dimensional problem can be obtained from the value of the wave function and its derivative at one point). We can then define the wave by two parameters, the values

p_0 of the pressure and u_0 of the acoustical velocity in a reference plane that we choose at the end of the neck (the plane where we wish to measure the impedance). By continuation of the solution towards the inside of the measurement head, one can obtain the acoustical wave everywhere inside the head, and in particular write the signals s_1 and s_2 provided by the two microphones as linear functions of p_0 and u_0 :

$$\begin{cases} s_1 = \alpha p_0 + \beta \rho c u_0 \\ s_2 = \gamma p_0 + \delta \rho c u_0 \end{cases} \quad (27)$$

where α, β, γ and δ are unknown parameters that depend on the geometry of the system, as well as on the gain of the microphones.

We have

$$Z_{in} = p(0)/u(0) = p_0/u_0. \quad (28)$$

Let us now define

$$y = \frac{s_2}{s_1} = \frac{\gamma Z_{in} + \delta \rho c}{\alpha Z_{in} + \beta \rho c}. \quad (29)$$

We now have

$$Z_{in} = \rho c \frac{Ay + B}{y - y_0}, \quad (30)$$

where $A = -\beta/\alpha, B = \delta/\alpha$, and $y_0 = \gamma/\alpha$ are three unknown constants to be determined. These constants are determined by the phase of calibration. Since there are three constants, three different measures of known impedances will be necessary. The most logical impedance to use is an infinite impedance, that is simply closing the head by a rigid surface in the reference plane. By doing this, we obtain directly y_0 . Then, two reference cavities with known impedances Z' and Z'' are used and the corresponding values y' and y'' are measured. After some calculations, we have

$$Z_{in} = \rho c \frac{\overline{Z}'(y' - y_0)(y - y'') + \overline{Z}''(y'' - y_0)(y' - y)}{(y - y_0)(y' - y'')} \quad (31)$$

where bars over the impedances denote normalized impedances (normalized by $Z_c = \rho c$).

That relation is the key of the TMTC method, since it gives the input impedance depending on the ratio of two microphone signals. What is remarkable in that method is that the measurement head does not need to be totally cylindrical. The important thing is that the neck of the head (near the reference plane) needs to be cylindrical, to be sure we have a one-dimensional propagation.

Like Laloë and Gibiat explain, “although in principle two microphones are sufficient, in practice it is useful (if

not indispensable !) to have more, three or even four”. We will not present here all aspects of that point, but the idea is that each pair of microphones cover a certain range of frequencies with reliability and accuracy.

Furthermore, care has to be taken about signal levels, since too low a level will induce a bad signal-to-noise ratio, and too high a level will induce non-linearities.

B. Experimental setup

Our experimental setup is shown on Figure 19. It consists of a measurement head into which six microphones are inserted. At one end, a loudspeaker can excite the interior of the head. At the other end of the head, an adaptor enables an acoustic component to be attached, a mouthpiece in our case. The microphones are connected to a sound card and a computer. A MATLAB interface facilitates calibration and measurement performance.

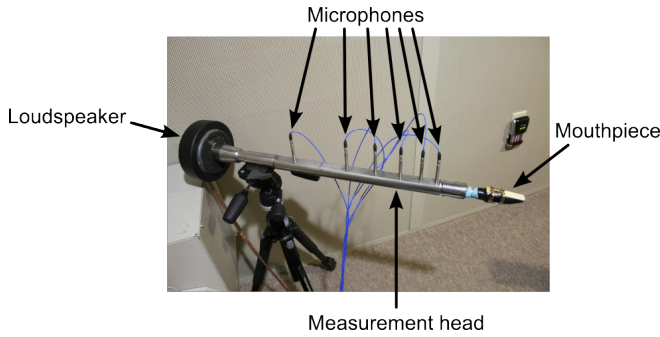


Figure 19. Experimental setup : six microphones are inserted in a measurement head. At one end, a loudspeaker can excite the air inside the head. At the other end, a mouthpiece can be attached. The microphones are linked to a computer interface. A MATLAB interface facilitates calibration and measurement performance.

Each mouthpiece was inserted so that the end of the mouthpiece reached the same position on the adaptor. The mouthpiece measurements were completed by inserting each of the mouthpieces so that the base lined up to a common spot on the mouthpiece adaptor. But since the mouthpieces were not inserted up to the reference plane, the measured impedance Z_{meas} is not exactly the input impedance of the mouthpiece Z_{mouth} (see Figure 20).

Indeed, there is a cylindrical section of length L , which we need to “remove” from the measured impedance, in order to get the impedance of the mouthpiece. For this purpose, we use equation (10) adapted to our case, that is :

$$Z_{meas} = Z_c \frac{Z_{mouth} \cos(kL) + jZ_c \sin(kL)}{Z_c \cos(kL) + jZ_{mouth} \sin(kL)}. \quad (32)$$

from which we can obtain the normalized input impedance of the mouthpiece

$$Z_{mouth}/Z_c = \frac{jZ_c \sin(kL) - Z_{meas} \cos(kL)}{jZ_{meas} \sin(kL) - Z_c \cos(kL)} \quad (33)$$

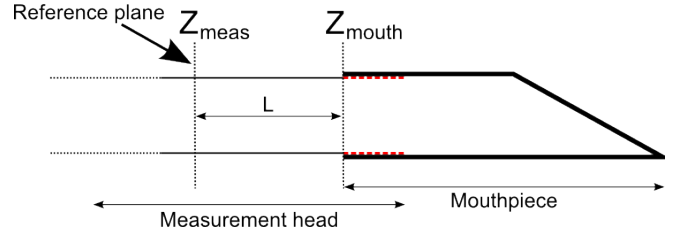


Figure 20. Schematic view of the mouthpiece at the end of the measurement head. The measured impedance Z_{meas} is not directly the input impedance Z_{mouth} of the mouthpiece : there is a cylindrical section of length L added we need to take into account.

or

$$\bar{Z}_{mouth} = \frac{j \sin(kL) - \bar{Z}_{meas} \cos(kL)}{j \bar{Z}_{meas} \sin(kL) - \cos(kL)}. \quad (34)$$

C. Results and discussion

Figures 21 and 22 present comparisons between the measured and computed input impedances. Table III gives comparisons between the first two resonant frequencies for each mouthpiece.

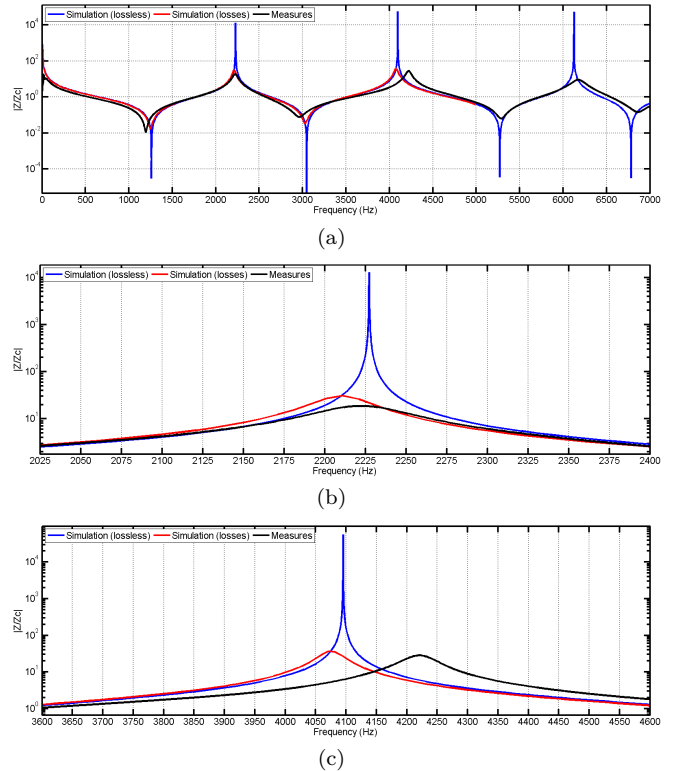


Figure 21. (a) Comparison between the computed and measured input impedance of the Selmer mouthpiece. (b) Zoom around the first resonance. (c) Zoom around the second resonance.

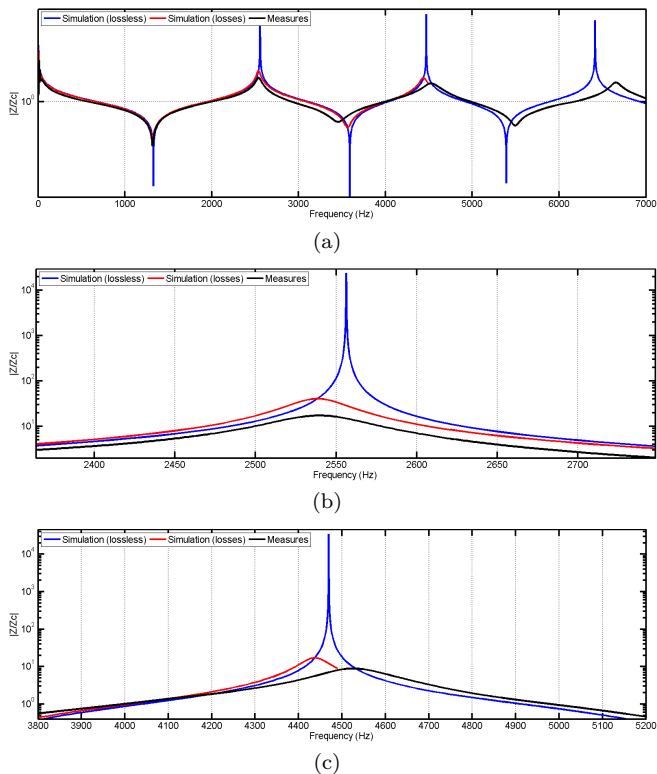


Figure 22. (a) Comparison between the computed and measured input impedance of the Lebayle mouthpiece. (b) Zoom around the first resonance. (c) Zoom around the second resonance.

		First resonance (Hz)	Second resonance (Hz)
Selmer	Simulation (lossless)	2227	4095
	Simulation (losses)	2210	4075
	Measures	2222	4222
Lebayle	Simulation (lossless)	2556	4469
	Simulation (losses)	2539	4437
	Measures	2539	4526

Table III. Comparison between the measured and simulated first two resonant frequencies for the two mouthpieces.

Our simulations seem in good agreement with the measurements. Of course, the resonant frequencies are not exactly resolved, but the relative maximum error for the two first resonant frequencies is around 10^{-2} , which seems fairly good since we had to model the mouthpieces manually. Furthermore, we can notice that the higher the frequency is, and the more discrepancies there are. This seems logical, since higher frequencies are more sensitive to a higher level of detail of the geometry of the mouthpiece.

Finally, it appears that accessing more precise simulations only requires better models of the mouthpieces.

V. CONCLUSIONS AND PERSPECTIVES

During this internship, we validated a method based on finite element method to compute the input impedance of saxophone mouthpieces, seen from the back of the mouthpiece. In order to validate the method to compute input impedances, measurements were done thanks to the TMTC method. Even if there are discrepancies between measurements and simulations, particularly as we go into high frequencies, it appeared that “handmade” models of the mouthpieces gave fairly good results, and that we can be confident about the method. If one is seeking more confidence in the method, he will simply need to have access to more precise geometry data for the models.

The next step is then to use that method to compute the “real” input impedances of mouthpieces, that is impedances seen from the side of the mouth (which is the “real” side of excitation). Even if it is quite easy to change the exciting side of the mouthpiece on the computer (contrary to measurements), questions still hold about how exactly the mouthpiece is excited in playing conditions.

Furthermore, the roles of turbulence in the air flow in the mouthpiece and vibration of the reed (particularly its coupling with air) are not yet clear. This present work could potentially be continued on COMSOL, using the module “Aeroacoustics”, in order to study the air flow, or the “Structural Mechanics”, in order to couple it with the “Acoustics” module and take into account the motion of the reed during sound production.

Finally, from a more personal point of view, this internship was a real opportunity to mix two passions : music (as a saxophonist !) and physics. This is a great chance. I had the opportunity to meet a lot of “scientific people” interested in music, and discovered areas of research I never heard of before (do you know what is the Ballagumi ?).

Acknowledgments

First of all, I would like to thank Gary Scavone – my internship advisor – who gave me the opportunity to work in his lab, in such good conditions, and to work on such an interesting subject. Even if the autonomy he left me was enjoyable, Gary was always there when needed, and his wise advice was really appreciated. Next, I want to thank Antoine Lefebvre, who first worked on my subject with Gary, then needed to leave the lab, but continued to give some help. The precious time he dedicated to help me with the first steps with COMSOL saved me a lot of time. Darryl Cameron, working at MusicTech (McGill), Julien Boissinot working at CIRMMT, Maxime Boissoneault and Félix-Antoine Fortin, both working at CLUMEQ/Compute Canada must be infinitely thanked, since they dedicated to me a lot of time in order to make COMSOL working on Colosse. For their help for creating the mouthpieces models, I wish to thank Alain Batailly and Juan Henao. Finally, this work was supported in part by a grant from the Natural Sciences and Engineering

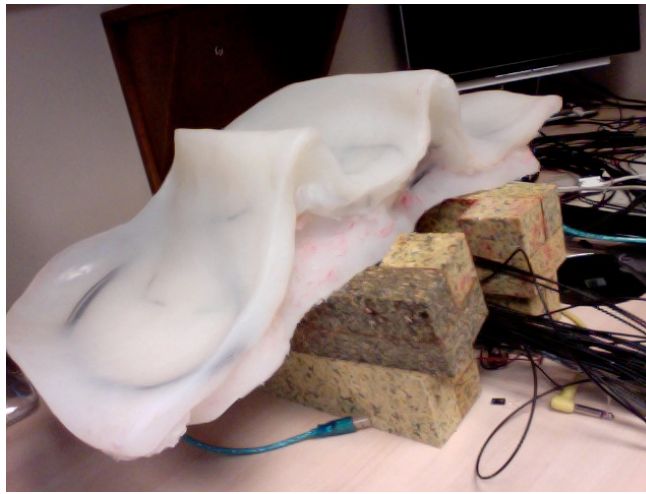


Figure 23. The Ballagumi

Research Council (NSERC) of Canada, RGPIN 298321-10.



McGill



compute+calcul
CANADA



NSERC
CRSNG

- ¹ Claudia Fritz, Joseph Curtin, Jacques Poitevineau, Palmer Morrel-Samuels, and Fan-Chia Tao. Player preferences among new and old violins. *Proceedings of the National Academy of Sciences*, January 2012.
- ² Gary Scavone. *An Acoustic Analysis of Single-Reed Woodwind Instruments with an Emphasis on Design and Performance issues and digital waveguide modeling techniques*. PhD thesis, Stanford University, Stanford, CA, 1997.
- ³ John Backus. Input impedance curves for the reed woodwind instruments. *The Journal of the Acoustical Society of America*, 56(4):1266, 1974.
- ⁴ Jean-Pierre Dalmont, Marthe Curtit, and Ahmad Fazli Yahaya. On the accuracy of bore reconstruction from input impedance measurements: application to bassoon crook measurements. *The Journal of the Acoustical Society of America*, 131(1):708–714, January 2012. PMID: 22280692.
- ⁵ Allan D. Pierce. *Acoustics: An Introduction to Its Physical Principles and Applications*. American Institute of Physics, December 1989.
- ⁶ TOP500 project. <http://i.top500.org/stats>.
- ⁷ PAFI, plateforme d'Aide à la facture instrumentale. <http://www.pafi.fr/>.
- ⁸ Pauline Eveno, Jean-Pierre Dalmont, René Caussé, and Joël Gilbert. Wave propagation and radiation in a horn: Comparisons between models and measurements. *Acta Acustica united with Acustica*, 98(1):158–165, 2012.

- ⁹ Pauline Eveno, Jean-Pierre Dalmont, René Caussé, and Joël Gilbert. Comparisons between models and measurements of the input impedance of brass instruments bells. pages 567–572, Aalborg, Denmark, 2011. European Acoustics Association,.
- ¹⁰ Paul Dickens, John Smith, and Joe Wolfe. Improved precision in measurements of acoustic impedance spectra using resonance-free calibration loads and controlled error distribution. *The Journal of the Acoustical Society of America*, 121(3):1471–1481, March 2007. PMID: 17407884.
- ¹¹ Alexander Buckiewicz-Smith. *Methods for measuring the acoustic response of wind instruments*. PhD thesis, McGill, Montréal, February 2008.
- ¹² Jean-Pierre Dalmont. Acoustic impedance measurement, part i : A review. *Journal of Sound Vibration*, 243:427–439, June 2001.
- ¹³ Vincent Gibiat and Franck Laloë. Acoustical impedance measurements by the two-microphone-three-calibration (TMTTC) method. *The Journal of the Acoustical Society of America*, 88(6):2533–2545, 1990.